https://doi.org/10.17163/abyaups.49.382

Effect of Post-Heating on SMAW-Welded A-42 Grade Steel Rods

Cristian Leiva-González
Universidad Politécnica Salesiana, Ecuador
Orcid: https://orcid.org/0000-0002-8255-1337

Jorge Muñoz-Paredes
Universidad Politécnica Salesiana, Ecuador
Orcid: https://orcid.org/0009-0005-2453-1943

Steven Celi-Jiménez
Universidad Politécnica Salesiana, Ecuador
Orcid: https://orcid.org/0009-0009-9233-6532

William Quitiaquez-Sarzosa
Universidad Politécnica Salesiana, Ecuador
Orcid: https://orcid.org/0000-0001-9430-2082

Introduction

Within the construction field, several methods are used for joining structural steel rods, one of them is welding, this study AWS D1.4 standard is use. The problems in welding A-42 rods are cracks in the area affected by heat, the structural rods have a low carbon content and the presence of elements such as Manganese, Silicon, Molybdenum, Chromium, Vanadium, Nickel, and Copper in their chemical composition. Low carbon steels have a percentage lower or equal to 0.41 % of Carbon Equivalent affecting the rod weldability since the carbon content is inversely proportional to the weldability of a material due to the fact that a martensitic structure was generate since when developing the weld bead, heat treatment temperatures are reached, which changes its microstructure (Niebles et al., 2014), (Rabiey et al., 2022). The austenite will transform into martensite, increasing the cracking in the weld bead, which occurs due to the hydrogen introduction, the martensitic structure will increase the hardness of the material at the expense of a reduction of its ductility, it which is detrimental to a structural application.

The present study seeks to avoid the formation of the martensitic microstructure by post-heating after welding, and at the same time to relax the residual stresses caused by the high temperatu-

res of the welding process. This hydrogen cracking occurs due to thermal contractions during the cooling of the weld since it is cooled to temperatures below 200 °C, producing high rates of stresses in the weld area this originates since some zones are at different temperatures generating compressions and tension in the weld bead (Messler, 1999 Huang, B. et al., 2020). The post-heating process consists of cooling the welded joint to a specific temperature and time higher than the beginning of the martensitic transformation, these values was obtained from Temperature-Time-Transformation Diagrams, these diagrams are also known as S-Curve (Batista-Suárez et al., 2018).

Olabi y Hashmi (1995) investigated the effect of post welding by analyzing the mechanical properties and residual stresses of welded sections of type I structural steel beams. A 70 % reduction in residual stresses and a 15 % improvement in toughness were obtained, generating a decrease in tensile strength. (Zhang et al., 2018) used instrumented indentation test and finite element analysis based on microstructure to study the post weld effect and mechanical properties of weld metal. The author found that Post Weld Heat Treatment (PWHT) significantly influences in the weld metal mechanical properties, weld metal strength decreases after PWHT; the critical fracture toughness of weld metal significantly decreases after treating at 400 and 600 ºC and slightly decreases after treating at 700 ºC.

Krishnan (2002) conducted a study of Post Weld Heat Treatment of friction stir welds was carried out at solubilization temperatures of 520, 540 and 560 °C, followed by aging at 175 or 200 °C. The weld region exhibited very coarse grains after PWHT, and the hardness was evenly present on the surface. The naturally aged weld joining efficiency reached 72 % after 14 days. (L. Wang et al., 2018) studied the influence of laser welding parameters on the microstructure and mechanical properties of welded joints of 2A14-T6 alloy. It was showing that the tensile strength and elongation of the laser disk welded joint firstly increase and then decrease with increasing heat input. The fracture type in all specimens is define as ductile fracture. When the heat input is 75 kJ/m, the maximum tensile strength of the weld is 261.7 MPa, approximately 61.2 % of the base metal. (Joshi et al., 2023) studied the effect of post-weld heat treatment on the mechanical properties of friction stir welded 7075-T651 Aluminum alloy. A marginal reduction in ductility of about 17-20 % after post heat treatment in the welded specimens found. No reduction in the modulus of elasticity was observed in the base and welded metals.

This paper is divided as follows. Section 1 covers the Introduction where hydrogen cracking in welding is analyzed in addition, a state-of-the-art analysis has been placed. The second section shows the Materials and Methods used in the research, which developed through tests, standards,

and mathematical models for the data characterization. Section 3 analyzes the results obtained quantitatively and comparative graphs. The conclusions section analyzes the results obtained to establish the behavior of post-heating in welding.

Materials and Methods

The NTE INEN 2167 standard presents the percentages of carbon equivalent of the rebars, which is between 0.50 - 0.55 % (INEN NTE 2635, 2012). To obtain accurate data on the chemical composition of the rods, the spectrometry test was performing to obtain the equivalent carbon of the rods; this equivalent carbon value is a measure of the weldability of the steel. On the other hand, through the equivalent carbon, the TTT diagram suitable for post-heating is obtained.

Preparation of the Specimens

To know the chemical composition of the A-42 rods, spectrophotometry was developing, starting with the cutting of the rod at a length of 30 mm, since the length must be greater than 10 mm so that there is no error in the test. Once the cut is made, the surface face of the rod is sanded with abrasive sandpaper. Three sanding sequences are performed with sandpaper # 180, 200, 800 and 1200 in that order, to obtain flat and polished faces. The study was carried out with a sample of 5 specimens of each brand, since according to INEN 2635:2012, a tensile study should carry out several specimens greater than or equal to 5 (Kalpakjian & Schmid, 2014).

Spectrophotometric Test

Once the specimens had their faces completely flat, the spectrophotometry test was performing in the optical emission spectrophotometer of the Salesian Polytechnic University, which has a spectral range of 130-180 nanometers. It should be considered that the initial values given by the spectrophotometer may have errors in the range of 0.1-0.2 %, this reason, several burnings should carry out until the measurement was stabilized (Maigua et al., 2020).

The chemical composition was obtaining by spectrophotometry, the results are show in Table 1, where each rod that was examining complies with the Carbon Equivalent (CE) standard proposed by the standard INEN 2197 Ecuadorian, which should be between 0.50-0.55 % of CE.

Table 1
Chemical composition and EC for each brand of rod

Chemical Element	Rod A (%)	Rod B (%)	Rod C (%)
Carbon	0.286	0.30	0.275
Manganese	1.35	1.2	1.37
Silicon	0.0989	0.0832	0.0950
Chromium	0.0730	0.0781	0.0736
Molybdenum	0.0061	0.0052	0.0060
Vanadium	0.0011	0.0016	0.0005
Nickel	0.0390	0.031	0.0388
% CE	0.55	0.53	0.54

Obtaining the amount of EC presented by the rods and the carbon percentage of each one of them, the weldability was found by drawing a perpendicular line from the axis of X (EC) and Y (Carbon Percentage), where the lines coincide will be the weldability zone in Figure 1, the weldability of the rods can be observed (Phillips, 2016).

Figure 1
Weldability zone of rebars

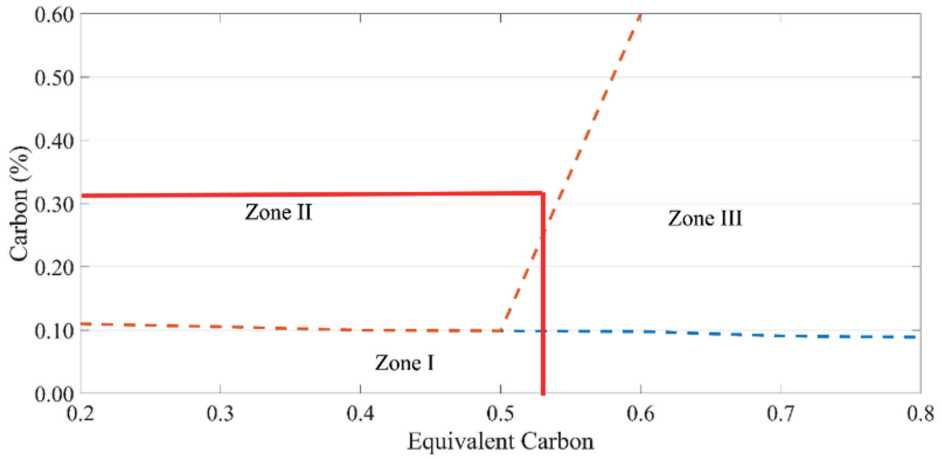

Note. Phillips, 2016

The weldability of the rods was finding in zone II, where there are cracks in the HAZ. The TTT diagram is selected based on the equivalent carbon content of the rod. Through spectroscopy test, and carbon average value of 0.55 % was obtained, for each rod brand (Singh, 2012). TTT diagram was used to perform the post-heating is shown in Figure 2 (Huang, X. et al., 2020). Likewise, the

post-heating cycle can observe, for this study the cooling from the solidification temperature of the weld bead to a temperature of 420 °C is performed, this to prevent the formation of martensite and to know the results for a maintenance temperature of 420 °C during a time of 30 min.

Figure 2
TTT diagram for 0.3 % carbon steel

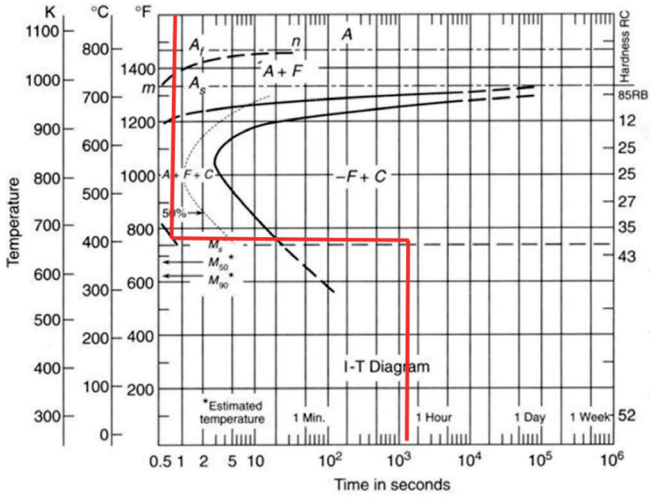

Note. Vander Voort, 1991

Obtained the rods chemical composition, the EC was calculate using Equation 1 of AWS D1.1 2020 (American Welding Society et al., 2020).

$$CE = C + \frac{Mn + Si}{6} + \frac{Cr + Mo + Cb + V}{5} + \frac{Ni + Cu}{15} \quad (1)$$

Figure 3 shows the post-heating process to is performed on the rods.

Figure 3
Post-heating process

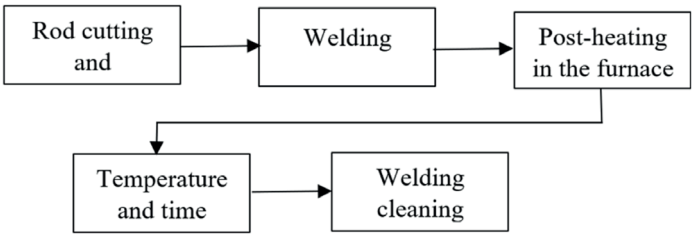

Equation 2 (Messler, 2008) was considering for the calculation of solidification time

$$S_t = \frac{L_f H_{net}}{2\pi K \rho C_p (T_m - T_o)} \quad (2)$$

Where St solidification time, Lf is the latent heat of fusion per unit volume, Sb the standard deviation, n the number of degrees of freedom, K the thermal conductivity of the base metal, ρ the density of the base metal, Cp the specific heat, Tm the melting temperature and To the initial temperature. The parameters used to determine the post heating cycle are voltage, current intensity and welding speed, values of 75 V, 120 A and 10mm/s, respectively. The steel physical properties with medium carbon content are specifying in Table 2.

Table 2
Physical properties of low carbon steel

Physical properties of low carbon steel at 20 °C	
Density [ρ]	7833 kg/m^3
Specific Heat [Cp]	465 J/kg·K
Diffusivity [x10^{-5}]	1.474 m^2/s
Thermal Conductivity [k]	54 W/m·K

The amount of heat (Lf) required to melt a given metal of volume is determined using Equation 3.

$$L_f = \frac{(T_m + 273)^2}{300000} \quad (3)$$

Obtaining a solidification time of 3 seconds, the time in which the solder solidifies, the solder well temperature reaches 1650 °C or more (Groover, 2014). Therefore, since the solder solidifies in 3 seconds, it is considered to enter the melting temperature. Figure 4 details the post-heating process that the corrugated rods will undergo.

Figure 4
Post-heating cycle

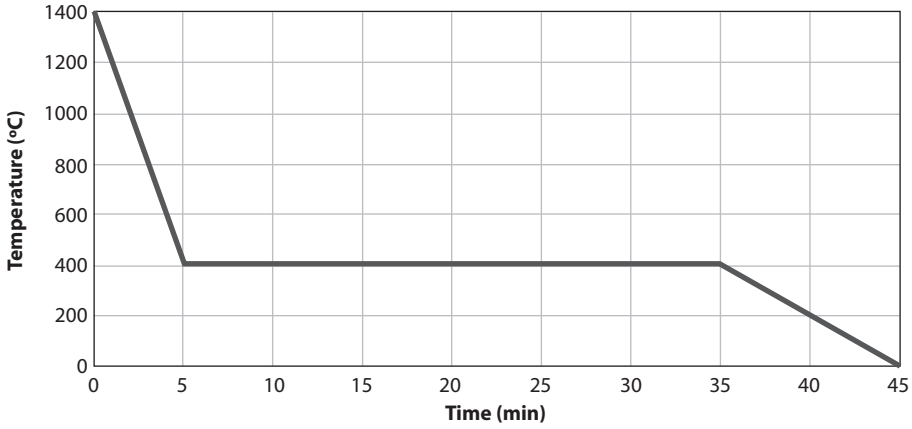

Subsequently, the t-student statistical analysis was applying for the tensile and hardness tests, which allows examining if there is a significant variation between the averages of two groups by hypothesis, which in this case has a group with post heating and another without post heating, to affirm or deny the hypothesis Equation 4 is used (Bravo, 2017), (Wang et al., 2021).

$$t = \frac{\bar{d}}{\frac{S_d}{\sqrt{n}}} \tag{4}$$

Where d is the differences Mean, Sb is the differences deviation and n the degrees of freedom number. To find the differences average equation 5 is applied (Bravo, 2017).

$$\bar{d} = \frac{\sum (d_{\text{without post}} - d_{\text{with post}})}{n} \tag{5}$$

Where d is the differences average, with post is the samples average without post-heating, and without post is the samples average with post-heating. The standard deviation of the differences is found by Equation 6 (Bravo, 2017).

$$S_b = \sqrt{\frac{(d_i - \bar{d})^2}{n-1}} \tag{6}$$

The freedom degrees (v) were founding using Equation 7.

$$v = n - 1 \tag{7}$$

As a result, it was founding that the critical value for two-tailed is 2.776.

Results and discussion

In this section the results obtained in the tensile and hardness tests are presented, which help to identify the changes in the weld mechanical properties.

Results of A-rods

Figure 5 presents the results of the ultimate strength obtained in the tensile tests. There is a reduction in the breaking strength of the A rods with post-heating with a maximum value of 420.15 MPa and a minimum of 300 MPa with respect to the maximum value, reduction was 6.08 %, and for the minimum value 55.44 %.

Figure 5
Dispersion of ultimate stress results for rod A

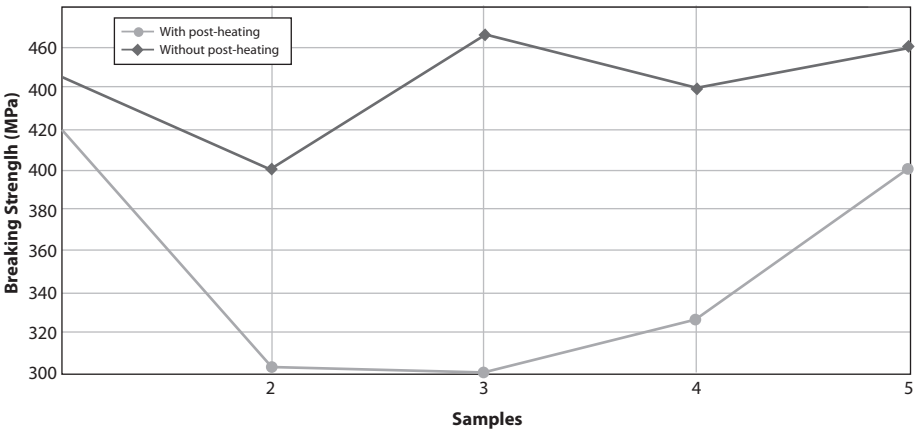

Figure 6 shows the results of the yield strength obtained in the tensile tests of the rods A. It can be observed in Figure 7. that there is a decrease in the yield strength of the rods A with post-heating, a maximum value of 393.5587 MPa and a minimum of 339.989 MPa is obtained, with respect to the maximum value the decrease was 1.64 % and for the minimum value it is 5.94 %.

Figure 6
Dispersion of yield strength results for rod A

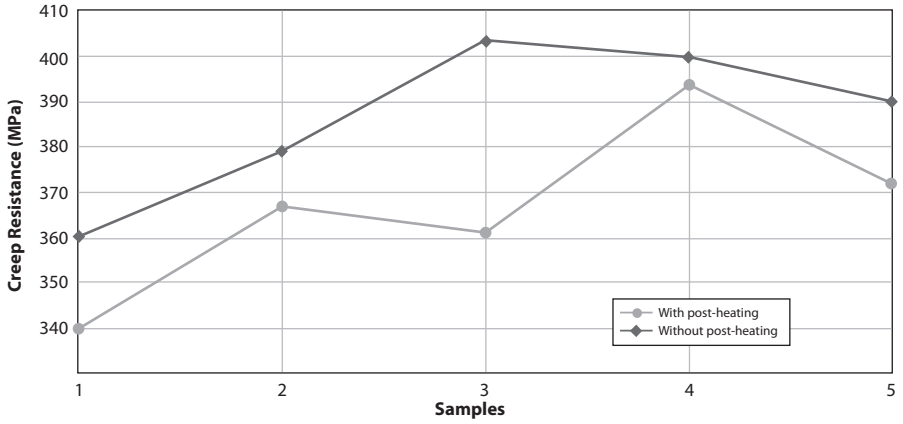

Figure 7 shows the dispersion of the results of the ultimate strength obtained in the tensile tests of the rods welded A, it is show in Figure 7. there is a reduction in the of the rods A ultimate strength with post-heating with a maximum and minimum value of 493.76 and 395.47 MPa, respectively. Relative to the maximum value the decrease was 5.69 %, and for the minimum value was 27.51 %.

Figure 7
Dispersion of ultimate strength results of rod A

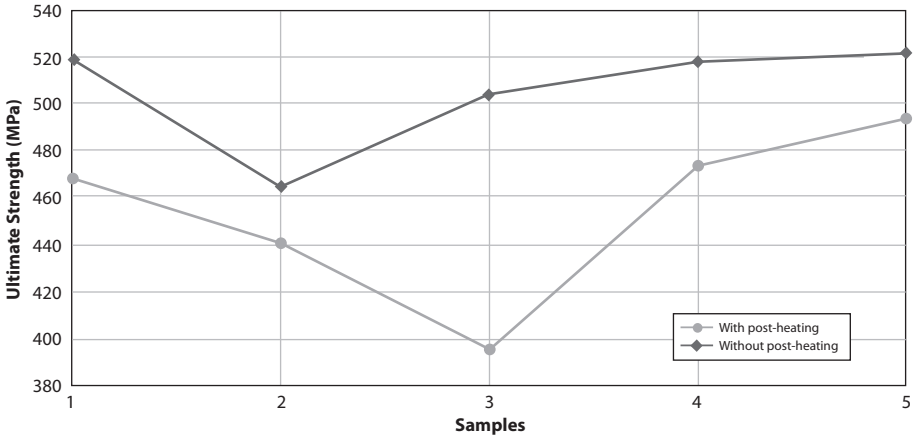

Figure 8 shows the hardness results at different positions of the polished surface of the A-rods. There is a decrease in the hardness of the rods A with post-heating with a maximum value of 78.7 MPa and minimum of 78 MPa with respect to the maxi-mum and minimum value decrease was 1.65 and 1.67 %, respectively.

Figure 8
Dispersion of hardness results of A-rods

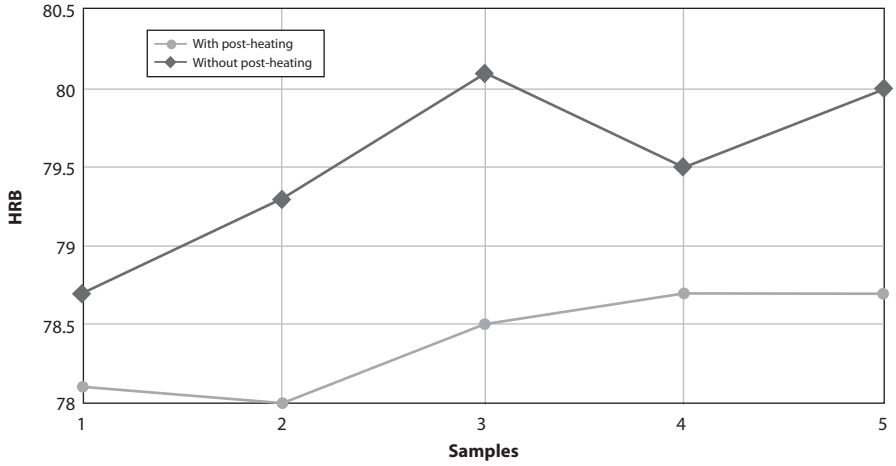

Table 3 shows the results of welded rods A ductility. There is an increase in the hard-ness of the A rods with post-heating with a maximum and minimum value of 25.35 and 17.85 %, respectively, with respect to the maximum value the increase was 53.54 % and for the minimum value was 2.94 %.

Table 3
Ductility results for rod A

ID Samples	With Post-heating Ductility (%)	Without Post-heating Ductility (%)
A 1	17.85	17.34
A 2	22.56	17.33
A 3	21.92	15.17
A 4	25.35	16.51
A 5	23.01	19.39

Results of B-rods

Table 4 shows the breaking strength results obtained in the tensile tests of welded rods type B for two groups, one with post-heating and the other without post-heating. There is an increase in the breaking strength of the B rods with post-heating with a maximum value of 500.01 MPa and a minimum of 432.55 MPa the increase the maximum value was 1.05 %, and for the minimum value, it was 1.67 %.

Table 4
Results of breaking strength of rod B

ID Samples	Rupture strength with post-heating (MPa)	Rupture strength without post heating (MPa)
B 1	468.96	486.35
B 2	479.75	458.12
B 3	495.82	494.18
B 4	432.55	380.09
B 5	500.01	450.25

Figure 9 shows the dispersion of the results of the yield strength with post-heating and without post-heating. There is an increase in the yield strength of rod B with post-heating with a maximum value of 458.95 MPa and a minimum of 415.67 MPa the increase the maximum value was 1.16%, and for the minimum value present a de-crease of 4.74 %.

Figure 9
Dispersion of yield strength results for rod

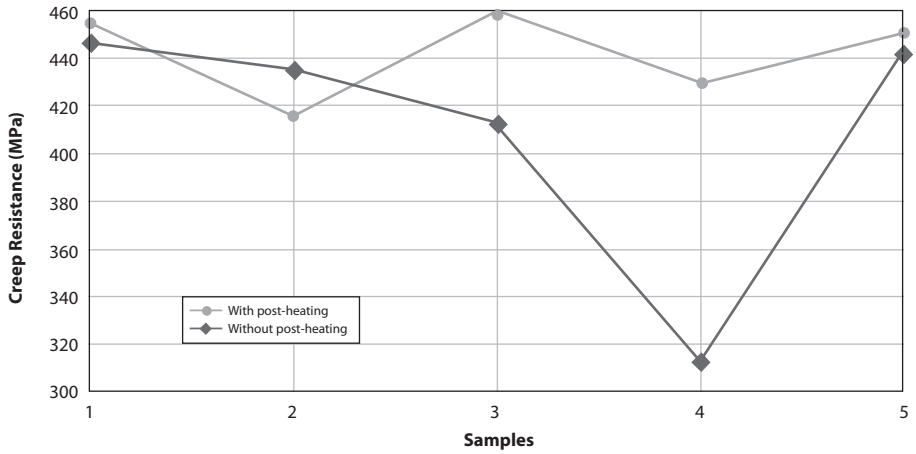

Figure 10 shows the results of the ultimate strength with post-heating and without post-heating. There is an increase in the ultimate resistance of the B rods with post-heating with a maximum value of 500.019 MPa and a minimum of 432.55 MPa the increase the maximum value was 11.05 %, and for the minimum value present a decrease of 13.8 %.

Figure 10
Dispersion of the results of the ultimate strength of the B rods

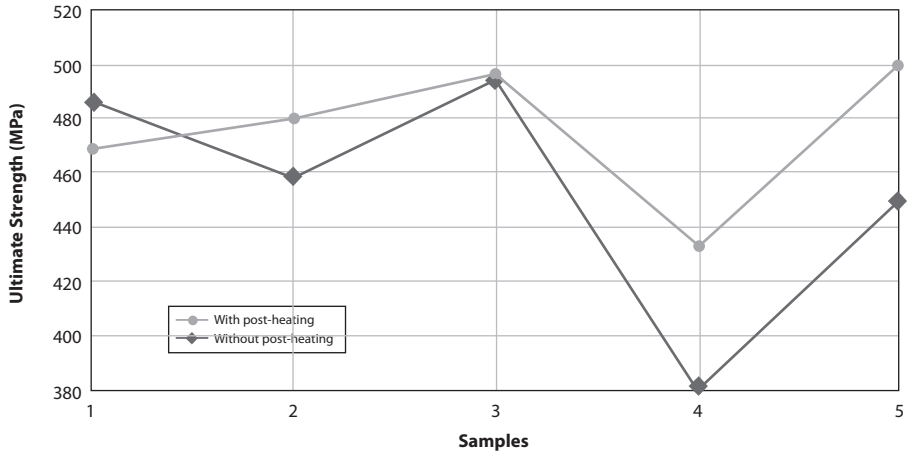

Figure 11 shows the hardness results at different positions of the polished surface of the B rods. A decrease in the hardness of the B rods with post-heating was evidencing with a maximum value of 76.8 HRB and a minimum of 68.1 HRB, the decrease the maximum value is 3.91 %, and for the minimum value, the decrease is 9.1 %.

Figure 11
Dispersion of hardness results of B rods

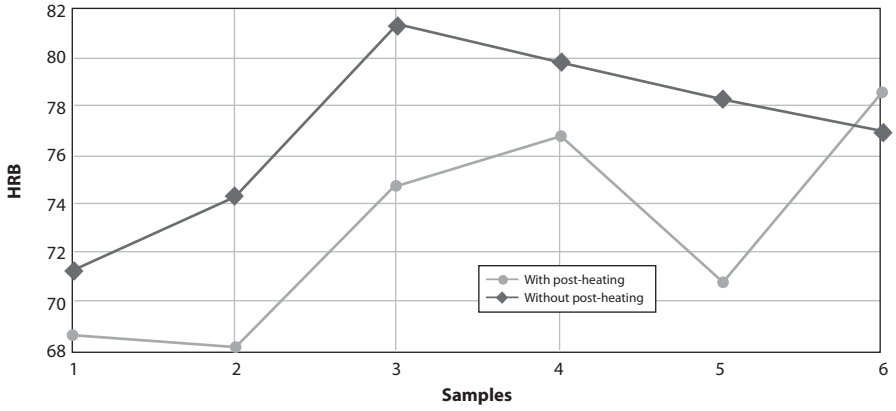

Figure 12 shows the results of ductility with and without post-heating. An increase in the ductility of the rods B with post-heating with a maximum value of 25.43 % and a minimum of 15.10 %, the increase the maximum value is 8.3 %, and the increase the minimum value is 7.86 %.

Figure 12
Dispersion of ductility results for B-rods

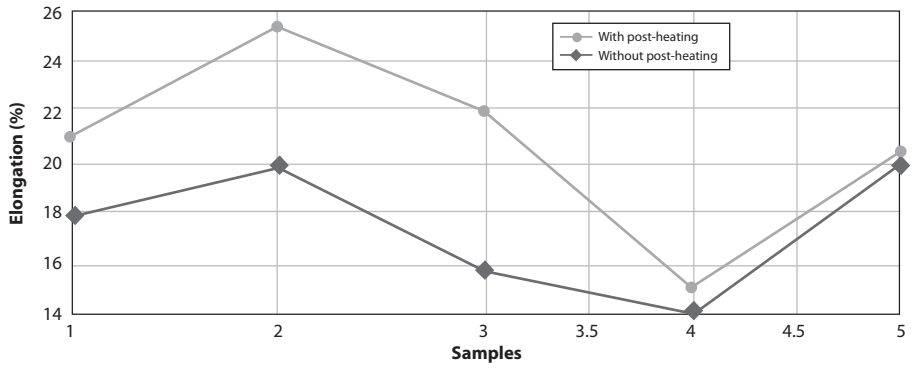

Results of C-rods

Figure 13. shows the breaking strength results obtained in the tensile tests of C welded rods for two groups, with post-heating and without post-heating. There is a decrease in the breaking strength of the C rods with post-heating with a maximum value of 449.01 MPa and a minimum of 422.64 MPa the maximum value is a singular point, there is an increase of 9.46 %, and for the minimum value, the decrease is 10.64 %.

Figure 13
Dispersion of results of the breaking strength of the rods C

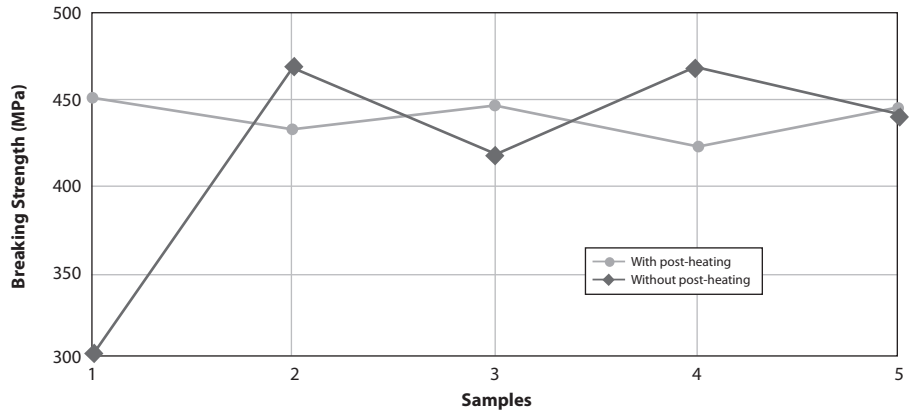

Figure 14. shows the yield strength results, which are obtained in the tensile tests of the C rods, for two groups with post heating and without post heating. It has observed an increase in the yield strength of the C rods with post heating with a maximum value of 431.6392 MPa and minimum of 412.47 MPa with

respect to the maximum value which is a singular point there is a decrease of 1.8 %, and for the minimum value the increase is 1.83 %.

Figure 14
Dispersion of yield strength results for C-rods

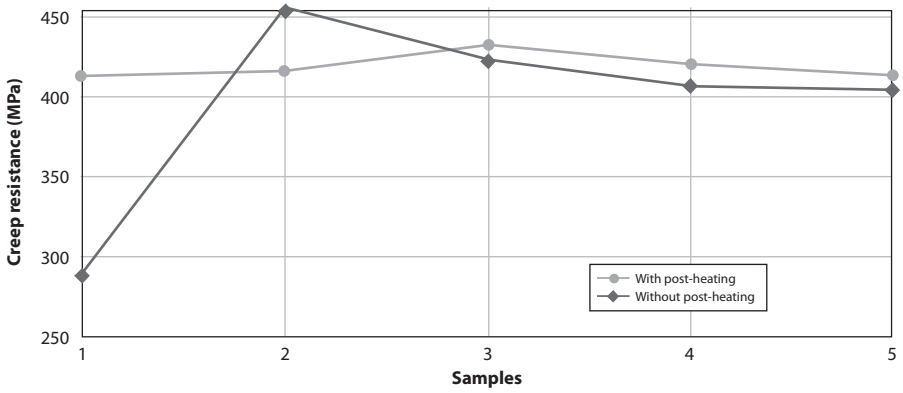

Figure 15 shows the results of the ultimate strength of the C rods with and without post-heating. There is a decrease in the ultimate resistance of the C rods with post-heating with a maximum value of 479.85 MPa and a minimum of 349.02 MPa to the maximum value, there is a decrease of 5.54 %, and for the minimum value is a singular point there is an increase of 40.7%.

Figure 15
Dispersion of the ultimate strength results of the C-rods

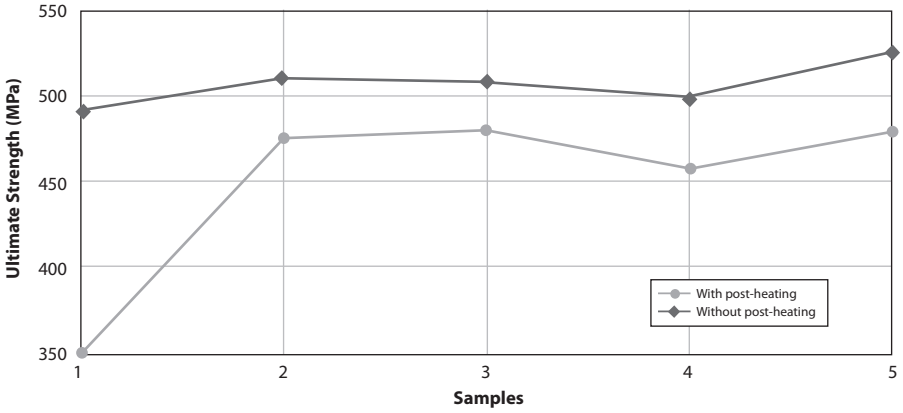

Figure 16 shows the hardness results at different positions of the polished surface of the C rods. There is a decrease in the hardness of the C rods

with post-heating with a maximum value of 65.5 HRB and minimum of 51.6 HRB to the maximum value there is a decrease of 11.73 %, and the decrease the minimum value is 11.73 %.

Figure 16
Dispersion of hardness results for C-rods

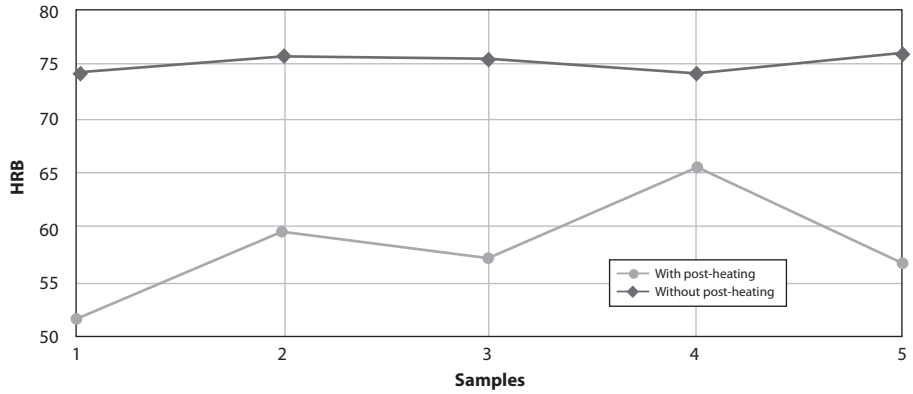

Figure 17. shows the results of ductility with and without post-heating. There is an in-crease in the rods C ductility with post-heating with a maximum value of 22.55 % and a minimum of 17.85 % the maximum value there is an increase of 20.59 %, and for the minimum value, the decrease is 12.83 %.

Figure 17
Dispersion of hardness results for C-rods

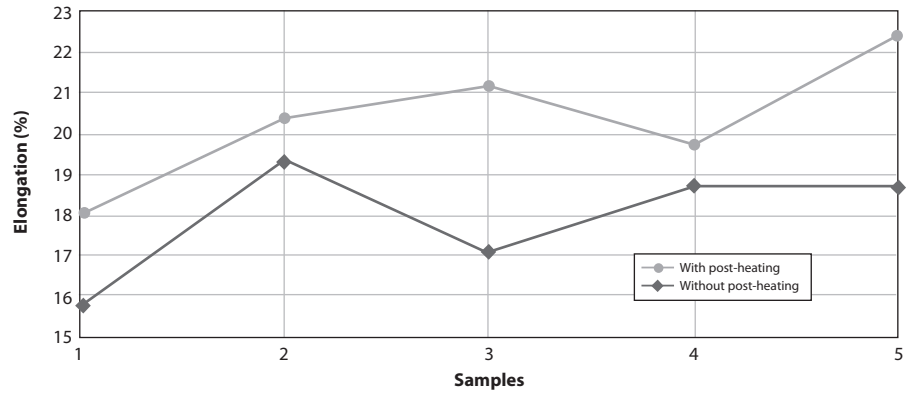

T-student test

The tensile and hardness tests Applying the statistical analysis t-student test for, it is analyzed if there is a significant variation between the averages of two groups utilizing the hypothesis that this case there is one group for the two cases in study. The following analysis is applied to the results of each rod (Quitiaquez Sarzosa et al., 2022).

Null Hypothesis for Stress and Hardness (H0): By performing a post-heating, stresses and hardness increase.

Alternate Hypothesis for Stress and Hardness (H1): After post-heating, strengths and hardness decrease.

Null Hypothesis for Ductility (HD0): Ductility decreases by performing a post-heating.

Alternate Hypothesis for Ductility (HD1): Ductility increases After post-heating. Table 5 presents the variables and the results obtained from the t-student analysis of the breaking strength of the A rods

Table 5
Variables and results obtained from t-student analysis for A ultimate strength

Variables	With post-heating	Without post heating
Mean	448.22	506.94
Variance	173.77	3155.06
Observations	5	5
Pearson correlation coefficient	0.75	
Hypothetical difference of means	0	
Degrees of freedom	4	
Statistic t	-2.78	
P(T<=t) one-tailed	0.024	
One-tailed value (one-tailed)	2.13	
P(T<=t) two tails	0.04	
Value-criticality (two tails)	2.77	

As presented in Figure 18, the t-statistic is established in the rejection zone, accepting the alternative hypothesis, which mentions when performing a post-heating, the resistances and hardness decrease.

Figure 18
T-curve to show zone of acceptance or rejection of the ultimate strength of the rods C

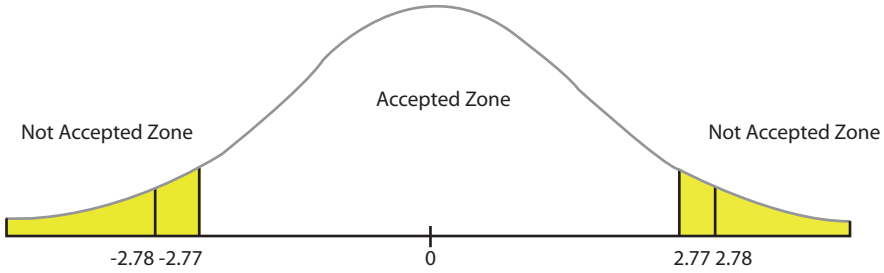

Note. Phillips, 2016

Table 6 shows the results of ultimate strength, creep and rupture, besides ductility and hardness of each rod brand, using the t-student test statistical analysis.

Table 6
Summary table of statistical analysis t-student test

Rod	Mechanical property	Similarity (%)	Accepted hypothesis
C	Ultimate Strength	4.9 %	The Alternate Hypothesis of Stress and Hardness (H1) is accepted: After post heating, stress and hardness decrease.
	Yield Strength	4.88 %	
	Breaking Strength	4.6 %	
	Hardness	1.7 %	
	Ductility	2.4 %	The Alternate Hypothesis Ductility (H1) is accepted: After post heating, ductility increases.
A	Ultimate Strength	2.8 %	The Alternate Hypothesis of Stress and Hardness (H1) is accepted: After post heating, stress and hardness decrease.
	Yield Strength	1.5 %	
	Breaking Strength	1.7 %	
	Hardness	1.5 %	
	Ductility	2.4 %	The Alternate Hypothesis Ductility (H1) is accepted: After post heating, ductility increases.
B	Ultimate Strength	3.3 %	The Alternate Hypothesis of Stress and Hardness (H1) is accepted: After post heating, stress and hardness decrease.
	Yield Strength	4.9 %	
	Breaking Strength	4.1%	
	Hardness	3.18 %	
	Ductility	4.8	The Alternate Hypothesis Ductility (H1) is accepted: After post heating, ductility increases.

Conclusions

By means of the statistical analysis t-student test, a decrease in the ultimate stress for rods C, A and B of 13.1, 11.22 and 11.43 % with a probability of error of 4.9, 2.8 and 3.3 %, respectively, was evidenced. Similarly, the yield stress decreases 14.91, 5.46 and 8.24 % with an error of 4.88, 1.5 and 4.9 %, ruptu-re with a decrease of 15.48, 26.47 and 13.46 % error of 4.6, 1.7 and 3.18 %, the hardness presents a de-crease of 21.32, 2.12 and 5.48 % with error percentages of 1.7, 1.5 and 3.18 %, having a level of reliability the 95 %.

Based on the t-student test, an in-crease for ductility was obtained for C, A and B of 17.64, 29.41 and 29.43 %, with an error probability of 2.4 % for C and A, with an error of 4.8 % and for rod B. Therefore, there is no martensite for-mation in the weld metal, and the weld seam does not suffer hydrogen cracking since hydrogen is scattered in the weld seam as a result of post-heating.

References

American Welding Society. Structural Welding Committee, American Welding Society. Technical Activities Committee, & American National Standards Institute. (2020). Structural welding code--steel. In *American Welding Society* (p. 634).

Batista-Suárez, Y., Fernández-Columbié, T. H., Rodríguez-González, I., & Leyva-Legrá, S. (2018). Transformaciones microestructurales en uniones soldadas de fundición nodular obtenidas por soldadura manual con electrodos austeníticos. *Minería y Geología, 34*(4), 470–484. https://n9.cl/gv7

Bravo, A. (2017). *Análisis del comportamiento de compra del producto varilla de construcción Novacero en la ciudad de Guayaquil.* [Trabajo de titulación Magíster en Gerencia de Marketing]. Universidad Catolica de Santiago de Guayaquil. https://n9.cl/jgozd5/

Groover, M. (2014). *Introduccion a los procesos de manufactura*. McGraw-Hill/Interamericana Editores, S. A https://n9.cl/d3f6x/

Huang, B., Liu, J., Zhang, S., Chen, Q., & Chen, L. (2020). Effect of post-weld heat treatment on the residual stress and deformation of 20/0Cr18Ni9 dissimilar metal welded joint by experiments and simulations. *Journal of Materials Research and Technology*, *9*(3), 6186–6200. https://n9.cl/55ft7

Huang, X., Wang, H., Xue, W., Ullah, A., Xiang, S., Huang, H., Meng, L., Ma, G., & Zhang, G. (2020). A combined machine learning model for the prediction of time-temperature-transformation diagrams of high-alloy steels. *Journal of Alloys and Compounds*, *823*, 153694. https://n9.cl/o5g3zINEN NTE 2635. (2012). *Método de ensayo para las propiedades de tracción de láminas plásticas delgadas*. Instituto Ecuatoriano de Normalización. https://n9.cl/enw4je/

Joshi, A., Gope, A., & Chandra Gope, P. (2023). Effect of post-weld heat treatment on mechanical properties and fatigue crack growth behaviour of friction stir welded 7075-T651 Al alloy. *Theoretical and Applied Fracture Mechanics*, *123*, 103714. https://n9.cl/x5sjj/

Kalpakjian, S., & Schmid, S. R. (2014). *Manufactura, Ingeniería y Tecnología*.

Krishnan, K. N. (2002). The effect of post weld heat treatment on the properties of 6061 friction stir welded joints. *Journal of Materials Science*, *37*(3), 473–480. https://n9.cl/86jv3/

Maigua, C., Quitiaquez, W., Simbaña, I., Quitiaquez, P., Toapanta-Ramos, F., & Isaza-Roldán, C. A. (2020). Diseño de un Sistema de Monitoreo de Vibraciones Mecánicas en Generadores

Hidroeléctricos de Media Potencia. *Revista Técnica Energía*, (17), 92-102.
Messler, R. (1999). Principles of Eelding: Processes, Physics, Chemistry, and Metallurgy. *Reservoir Engineering Handbook*, 909–1095. https://n9.cl/2p8m7/
Messler R. (2008). *Principles of Welding*. https://n9.cl/c7m6s (Original work published 2008)
Niebles, E. E., Unfried, J., & Torres, J. E. (2014). Metodologías para el estudio de soldabilidad en uniones soldadas. *Información Tecnológica*, *25*(1), 03-14. https://n9.cl/5e4w/0
Olabi, A. G., & Hashmi, M. S. J. (1995). The effect of post-weld heat-treatment on mechanical-properties and residual-stresses mapping in welded structural steel. *Journal of Materials Processing Technology*, *55*(2), 117-122. https://n9.cl/mzgin/
Phillips, D. (2016). *Welding engineering*. Wiley. https://n9.cl/lyl94/
Quitiaquez Sarzosa, R., Cocha, J., Quitiaquez, W., & Vaca, X. (2022). Investigation of geometric parameters with HSS tools in machining polyamide 6 using Taguchi method. *Materials Today: Proceedings*, *49*, 181–187. https://n9.cl/fxkd3/
Rabiey, M., Würsten, P., Senne, L., & Urban, L. (2022). The effect of pre- and post-heat treatment on hardness and residual stress by laser metal deposition process of tungsten carbide (Metco-Clad 52052) cladding on a CK45 substrate. *Procedia CIRP*, *108*, 205-209. https://n9.cl/9l6dj/
Singh, R. (2012). Applied Welding Engineering: Processes, Codes and Standards. In *Elsevier Inc* (1), 3-33
Vander Voort, G. F. (1991). Atlas of time-temperature diagrams for irons and steels. In *Carpenter Technology Corporation* (p. 766). ASM International.
Wang, L., Wei, Y., Zhao, W., Zhan, X., & She, L. (2018). Effects of welding parameters on microstructures and mechanical properties of disk laser beam welded 2A14-T6 aluminum alloy joint. *Journal of Manufacturing Processes*, *31*, 240–246. https://n9.cl/yr8uh/
Wang, J., Guo, X., Li, W., Wu, X., Zhang, Z., & Hancock, E. (2021). Statistical Mechanical Analysis for Unweighted and Weighted Stock Market Networks. *Pattern Recognition*, *120*, 108123. https://n9.cl/0v2x9/
Zhang, C., Yang, S., Gong, B., Deng, C., & Wang, D. (2018). Effects of post weld heat treatment (PWHT) on mechanical properties of C-Mn weld metal: Experimental observation and microstructure-based simulation. *Materials Science and Engineering: A*, (*712)*, 430–439. https://n9.cl/8cgu8/